SYNTHESIS AND CHARACTERIZATION OF LIMITED MIXED SODIUM MANGANESE - SODIUM COPPER SULFATE DIHYDRATES WITH A KRÖHNKITE-TYPE STRUCTURE AND THEIR ANHYDROUS ANALOGUES

Delyana Marinova[1], Mitko Georgiev[2], Tsvetelina Bancheva[2], Donka Stoilova[1]

[1]*Institute of General and Inorganic Chemistry*
Bulgarian Academy of Sciences, 1113 Sofia, Bulgaria
E-mail: d.manasieva@gmail.com
[2]*Department of Inorganic Chemistry*
University of Chemical Technology and Metallurgy
8 Kliment Ohridski, 1756 Sofia, Bulgaria

Received 01 October 2018
Accepted 20 November 2018

ABSTRACT

The investigations reported in this contribution were carried out with respect to possible application of the title solid solutions as precursors for the preparation of energy storage materials owing to their ability to store and transport sodium ions. On the basis of the solubility data combined with X-ray powder diffraction, it has been found that kröhnkite and Mn-krönhkite form limited solid solutions, irrespective of their isostructuness due to the different effective ionic radii of Cu^{2+} and Mn^{2+} ions, the difference in the lattice parameters of both kröhnkites, and the influence of the Jahn-Teller effect on the distortion of the MO_6 polyhedra. The solid solutions $Na_2Cu_{1-x}Mn_x(SO_4)_2 \cdot 2H_2O$ were characterized by means of X-ray powder diffraction, vibrational spectroscopy, TG-DTA-DSC and SEM methods. A new method for the synthesis of anhydrous sodium manganese copper sulfates is proposed. Two types of anhydrous solid solutions $Na_2Cu_{1-x}Mn_x(SO_4)_2$ and $Na_2Cu_xMn_{1-x}(SO_4)_2$ with saranchinaite and alluaudite-type structures, respectively, are obtained after heating the hydrated solid solutions at 350ºC. Additionally to the anhydrous solid solutions unidentified solid phases are obtained.

Keywords: kröhnkite-type solid solutions, solubility diagram, vibrational spectroscopy, phase transitions, X-ray powder diffraction.

INTRODUCTION

This contribution is a part of our several-years research on the formation and properties of solid solutions among the three dimensional double sulfates of 3d-transition metals with blödite- and kröhnkite-type crystal structures. The results are reported in our previous papers, as follows: limited blödite-type solid solutions $Na_2M_{1-x}Cu_x(SO_4)_2 \cdot 4H_2O$ (M = Co, Zn, Ni) are obtained by crystallization in the $Na_2Cu(SO_4)_2$–$Na_2M(SO_4)_2$–H_2O systems at 25ºC [1 - 4]; a continuous series of blödite-type solid solutions $Na_2Co_{1-x}Mg_x(SO_4)_2 \cdot 4H_2O$ is obtained by crystallization in the $Na_2Co(SO_4)_2$–$Na_2Mg(SO_4)_2$–H_2O system at 25ºC [5]; limited blödite- and kröhnkite-type solid solutions $Na_2Ni_{1-x}Mn_x(SO_4)_2 \cdot 4H_2O$ and $Na_2Mn_{1-x}Ni_x(SO_4)_2 \cdot 2H_2O$ are obtained by crystallization from the solutions containing manganese and nickel ions [6]. The compounds with blödite- and kröhnkite-type structures are attractive for scientists since they are considered to be used as precursors for the preparation of energy storage materials due to their ability to store and transport alkali ions [7 - 11 and Refs. therein]. For example, Marinova et al. reported that the alluaudite phase $Na_{2+\delta}Mn_{2-\delta/2}(SO_4)_3$ prepared from $Na_2Mn(SO_4)_2 \cdot 2H_2O$ demonstrates better electrochemical properties than the lithium manganese phospho-olivine $LiMnPO_4$ [9].

$Na_2Cu(SO_4)_2 \cdot 2H_2O$ (kröhnkite) and $Na_2Mn(SO_4)_2 \cdot 2H_2O$ (Mn-kröhnkite) belong to a large family of natural and synthetic compounds built up of kröhnkite-type octahedral-tetrahedral chains. According to the classification scheme proposed by Fleck et al. both salts crystallize in the structural type D [12, 13]. Recently, we have re-

ported the crystal structure of synthetic kröhnkite [4]. $Na_2Cu(SO_4)_2{\cdot}2H_2O$ and $Na_2Mn(SO_4)_2{\cdot}2H_2O$ crystallize in the monoclinic SG $P2_1/c$ (Z = 2) with the following lattice parameters: $Na_2Cu(SO_4)_2{\cdot}2H_2O$ - a = 5.812(1) Å, b = 12.650(3) Å, c = 5.516(2) Å, β = 108.38(1)º, V = 384.9 Å^3; $Na_2Mn(SO_4)_2{\cdot}2H_2O$ - a = 5.824(1) Å, b = 12.999(1) Å, c = 5.497(1) Å, β = 106.05(1)º, V = 399. 9 Å^3 (the structure of the manganese salt is reported in a previous paper of one of the authors (DS) [14]). The structures consist of $MO_4(H_2O)_2$ octahedra which share four corners with sulfate tetrahedra, thus forming chains $[M(SO_4)_2(H_2O)_2]$ along [001]. The chains are linked by Na^+ ions and hydrogen bonds, thus forming layers. Additionally, the latter form 3D structure through Na^+ ions and hydrogen bonds. The SO_4 tetrahedra act as polydentate ligands – they are involved in metal–oxygen bonds including Na^+ and M^{2+} cations. Both metal octahedra are distorted with respect to the M–O bond lengths (the distortion parameters Δ_{oct} have values of 0.01261 for kröhnkite and 0.00038 for Mn-kröhnkite; calculations are made according to Ref. [15]). The water molecules are linked to M^{2+} ions via the shortest M–O bond distances (bond lengths Cu–OH_2 and Mn–OH_2 have values of 1.9386 and 2.145 Å, respectively). The different M–O_W bond lengths in both compounds are responsible for the formation of hydrogen bonds of different strength due to the different metal–water interaction, i.e. to the different synergetic effect of the M^{2+} ions. The hydrogen bond strength as deduced from ν_{OD} of the matrix-isolated HDO molecules is reported in a previous paper of one of the authors (DS) [16]. Crystal structure of kröhnkite is shown in Fig. 1.

The present paper aims at studying the formation of solid solutions $Na_2Cu_{1-x}Mn_x(SO_4)_2{\cdot}2H_2O$ between the isostructural kröhnkite and Mn-kröhnkite in a wide concentration range ($0 < x < 1$) as a first step for the preparation of anhydrous solid solutions – materials for sodium batteries. For this purpose we have studied the solubility in the system $Na_2Cu(SO_4)_2$–$Na_2Mn(SO_4)_2$–H_2O at 25ºC. The advantage of the method used is the possibility to prepare homogenous solid solutions with desired compositions, which transform into anhydrous solid solutions after heating at comparatively low temperatures. The structural properties of solid solutions were characterized by means of X-ray powder diffraction, vibrational spectroscopy and SEM. The infrared and Raman spectra were interpreted in the light of the structure of the hydrates. The phase transitions, the enthalpies of dehydration and formation were monitored by means of thermal gravimetric method, differential thermal analysis, differential scanning calorimetry and X-ray diffraction at elevated temperature (HTXRD).

EXPERIMENTAL

$Na_2Cu(SO_4)_2{\cdot}2H_2O$ and $Na_2Mn(SO_4)_2{\cdot}2H_2O$ were prepared by crystallization from aqueous solutions according to the solubility in the ternary systems Na_2SO_4–$CuSO_4$–H_2O and Na_2SO_4–$MnSO_4$–H_2O at 25ºC [17]. The method of isothermal decrease of supersaturation was used to reach the equilibrium between the liquid and solid phases in the $Na_2Cu(SO_4)_2$–$Na_2Mn(SO_4)_2$–H_2O system at 25ºC (the different experimental steps of the method are reported in Refs. [1, 18]. The method used guarantees the receipt of homogenous solid solutions. Saturated solutions containing different ratios of the salts were vigorously stirred for 3-4 days. The concentrations of the sodium copper and sodium manganese sulfates in the aqueous solutions and solid solutions were determined, as follows: the copper ion concentration was determined iodometrically. The total concentration of the sulfate ions was determined after precipitation as $PbSO_4$ with $Pb(NO_3)_2$. The precipitate was dissolved in complexon III and Pb^{2+} were determined complexonometrically at pH 5.5-6 using xylenol orange as indicator. The concentration of the sodium manganese sulfate was calculated by difference. The method of Trendafelov and

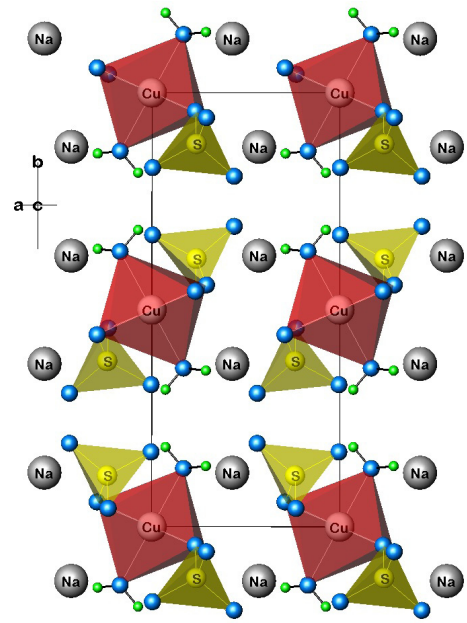

Fig. 1. Crystal structure of kröhnkite.

Balarew for an algebraic indirect identification of the solid phase compositions was applied to calculate the compositions of the completely dry solid solutions [19]. Anhydrous solid solutions were prepared by heating the hydrated samples at 350ºC for two days. The reagents used were ''p.a.'' quality. The distribution coefficients, describing the partitioning of the Cu^{2+} and Mn^{2+} ions between the liquid and solid solutions were calculated according to the equations:

$$D_{Cu/Mn} = C_{Cu(S)}C_{Mn(L)}/C_{Cu(L)}C_{Mn(S)}$$

and

$$D_{Mn/Cu} = C_{Mn(S)}C_{Cu(L)}/C_{Mn(L)}C_{Cu(S)}$$

where C are the concentrations in mass % of the copper and manganese ions in the liquid (L) and dry solid phases (S), respectively.

The infrared spectra were recorded on a Nicolet iS5 Fourier transform interferometer at ambient temperature over the frequency range of 4000 - 400 cm^{-1} (resolution < 2 cm^{-1}). The spectra were obtained using KBr discs as matrices. Ion exchange or other reactions with KBr have not been observed (infrared spectra using Nujol mulls were also measured). The Raman spectra were recorded with a Horiba Jobin-Yvon LabRAM HR800 spectrometer using a 600 l/mm grating and a 633 nm He-Ne laser line for excitation. The samples were placed under the 50x achromatic objective of an Olympus BX41 microscope and measured in back scattering configuration. The laser power on the sample was kept below 5.54 mW so that no heating and dehydration effects on the powder sample could be observed.

The X-ray powder diffraction data were collected within the range from 5° to 80° 2θ (step 0.02° 2θ, counting time 35 s/step) on a Bruker D8 Advance diffractometer with CuKα radiation and LynxEye detector. The lattice parameters of the anhydrous solid solutions were determined using the powder pattern calculation program FullProf Suite v.3.00 (Rodríguez-Carvajal, J., Satellite Meeting on Powder Diffraction of the XV Congress of the IUCr 1990, 127) and those of the anhydrous solid solutions with a program for least square unit cell refinements (LSUCR). The X-ray powder diffraction patterns at elevated temperature (temperature interval 25 - 400°C) were obtained using a PANalytical Empyrean equipped with a multichannel detector (Pixel 3D) using Cu Kα (45 kV-40 mA) radiation in the 10 - 100° 2θ range, with a scan step of 0.01° for 24 s. The high temperature X-ray diffraction measurements were carried out by means of an ANTON PAAR HT-16 camera with a sample directly heated with a heating filament. All experiments were performed on air (heating rate 5ºC per minute).

Simultaneous TG–DTA curves were obtained applying a computerized combined apparatus for thermal analysis LABSYSEvo, SETARAM Company, France, at atmospheric pressure in a flow of synthetic air (MESSER CHIMCO GAS – OOH 1056, ADR 2, 1A) in the temperature range 25 - 400ºC. Corundum crucibles with a volume of 100 µl were used. The sample weight in all tests was 50–60 mg. The experiments were carried out in dynamic mode, with heating rates of 5ºC min^{-1} and oxidizing gas flow rates of 20 ml min^{-1}. The DSC measurements were recorded on a STA PT1600 (TG-DTA/DSC Simultaneous Thermal Analysis) instrument in air up to 400 °C at a heating rate of 5°C min^{-1} using standard corundum crucibles (sample mass about 18 - 20 mg).

Scanning electron microscopy (SEM) of selected samples was performed on a JSM 6390 electron microscope (Japan) in conjunction with energy dispersive X-ray spectroscopy (EDS, Oxford INCA Energy 350) equipped with an ultrahigh resolution scanning system (ASID-3D) in regimes of secondary electron image (SEI). The accelerating voltage was 20 kV, I ~ 65 µA and the pressure was of the order of 10^{-4} Pa. The samples were gold coated with coating times of ~40 sec. The particles size is additionally measured with program LINCE-Linear Intercept v.2.4.2.

RESULTS AND DISCUSSION

Solubility diagram of the three-component $Na_2Cu(SO_4)_2$-$Na_2Mn(SO_4)_2$-H_2O system at 25ºC

The above system is studied from a saturated solution of the copper compound up to a saturated solution of the manganese one. The solubility diagram is shown in Fig. 2 and the experimental solubility data are summarized in Table 1. Two crystallization fields of solid phases are observed in the solubility diagram – a large crystallization field of solid solutions having kröhnkite as a matrix and a comparatively narrow crystallization field of solid solutions having Mn-kröhnkite as a matrix. The experiments show that the Mn-kröhnkite incorporates up to 16 mol % copper ions, while kröhnkite incorporates up to 8 mol % manganese ions. The solubility diagram

Table 1. Solubility in the $Na_2Cu(SO_4)_2$-$Na_2Mn(SO_4)_2$-H_2O system at 25ºC.

Liquid phase, mass%		Wet solid phase, mass%		Fully dried solid phase, mass%,		Liquid phase, mol parts		Solid phase, mol parts				Composition of the solid phases
NaCuS	NaMnS	NaCuS	NaMnS	NaCuS	NaMnS	Cu	Mn	Cu	Mn	$D_{Mn/Cu}$	$D_{Cu/Mn}$	
27.15	-	-	-	89.33	-	1.00	0.00	1.00	0.00	-	-	$Na_2Cu(SO_4)_2\cdot 2H_2O$
22.86	6.16					0.78	0.22					$Na_2Cu_{1-x}Mn_x(SO_4)_2\cdot 2H_2O$
16.00	13.81	64.36	6.27	85.75	3.58	0.53	0.47	0.96	0.04	0.05	-	$Na_2Cu_{0.96}Mn_{0.04}(SO_4)_2\cdot 2H_2O$
13.27	17.96	59.09	9.89	85.01	4.52	0.42	0.58	0.95	0.05	0.04	-	$Na_2Cu_{0.95}Mn_{0.05}(SO_4)_2\cdot 2H_2O$
11.37	21.78	61.00	10.51	83.10	6.15	0.34	0.66	0.93	0.07	0.04	-	$Na_2Cu_{0.93}Mn_{0.07}(SO_4)_2\cdot 2H_2O$
8.24	27.50	61.71	12.30	82.10	7.10	0.23	0.77	0.92	0.08	0.03	-	$Na_2Cu_{0.92}Mn_{0.08}(SO_4)_2\cdot 2H_2O$
8.01	28.21	46.76	27.97	61.45	27.88	0.22	0.78	0.68	0.32			eutonics
8.67	28.64	13.46	63.17	15.01	74.32	0.23	0.77	0.16	0.84	-	0.67	$Na_2Cu_{0.16}Mn_{0.84}(SO_4)_2\cdot 2H_2O$
6.32	30.97	9.52	67.57	10.50	78.82	0.17	0.83	0.12	0.88	-	0.69	$Na_2Cu_{0.12}Mn_{0.88}(SO_4)_2\cdot 2H_2O$
4.01	31.45	7.12	78.01	7.17	82.16	0.12	0.88	0.08	0.92		0.68	$Na_2Cu_{0.08}Mn_{0.92}(SO_4)_2\cdot 2H_2O$
3.05	32.53	4.73	70.84	5.01	84.32	0.11	0.89	0.06	0.94	-	0.63	$Na_2Cu_{0.06}Mn_{0.94}(SO_4)_2\cdot 2H_2O$
-	35.11	-	-	-	89.05	0.00	1.00	0.00	1.00	-	-	$Na_2Mn(SO_4)_2\cdot 2H_2O$

points a large miscibility gap extended from a solid solution $Na_2Cu_{0.92}Mn_{0.08}(SO_4)_2\cdot 2H_2O$ to a solid solution $Na_2Cu_{0.16}Mn_{0.84}(SO_4)_2\cdot 2H_2O$. The distribution coefficient of the manganese ions between the liquid phases and solid solutions $D_{Mn/Cu}$ has a mean value 0.04, while $D_{Cu/Mn}$ has a mean value of 0.66. X-ray powder diffraction patterns of the solid solutions are presented in Fig. 3 and the respective lattice parameters of the solid solutions are given in Table 2.

The experimental results point that irrespective of their isostructureness both kröhnkites form limited solid solutions owing to several reasons: (i) different effective ionic radii of Cu^{2+} and Mn^{2+} ions (0.73 Å vs. 0.83 Å); (ii) different lattice parameters *b,* β and unit cell volumes *V*, and (iii) the influence of the Jahn-Teller effect on the strong distortion of the CuO_6 polyhedra.

Vibrational spectra of neat double sulfates and solid solutions

The free tetrahedral ions (XO_4^{n-}) under perfect T_d symmetry are characterized with four internal vibrations, as follows: $\nu_1(A_1)$, the symmetric X–O stretching modes, $\nu_2(E)$, the symmetric XO_4 bending modes, $\nu_3(F_2)$ and $\nu_4(F_2)$, the asymmetric stretching and bending modes, respectively. The normal vibrations of the free sulfate ions in aqueous solutions are reported to appear, as follows: ν_1

Table 2. Lattice parameters of solid solutions $Na_2Cu_{1-x}Mn_x(SO_4)_2\cdot 2H_2O$.

Composition	*a*, Å	*b*, Å	*c*, Å	β, º	*V*, Å^3
x = 0 single crystals [4]	5.812(1)	12.650(3)	5.516(2)	108.38(1)	384.9
x = 0 this paper	5.818(1)	12.659(2)	5.510(2)	108.35(1)	385.3
x= 0.05	5.820(2)	12.669(3)	5.511(2)	108.35(2)	385.7
x= 0.07	5.823(1)	12.673(3)	5.513(1)	108.36(1)	386.2
x= 0.84	5.819(2)	12.954(1)	5.492(2)	106.28(1)	397.4
x= 0.88	5.819(3)	12.969(2)	5.491(2)	106.19(2)	398.0
x= 0.94	5.820(2)	12.983(3)	5.492(2)	106.12(2)	398.7
x= 1 this paper	5.818(2)	12.990(1)	5.493(3)	106.08(1)	398.9
x = 1 single crystals [14]	5.824(1)	12.999(1)	5.497(1)	106.05(1)	399. 9

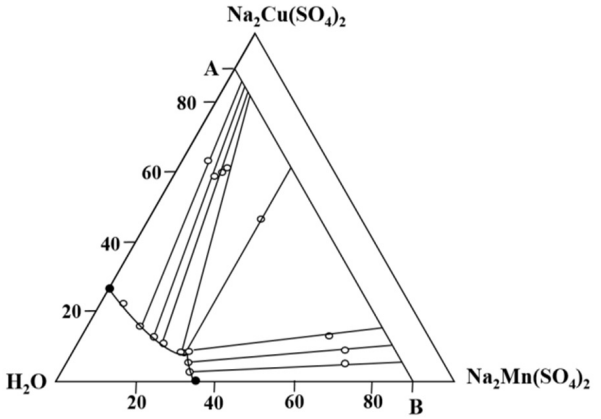

Fig. 2. Solubility diagram of the $Na_2Cu(SO_4)_2$–$Na_2Mn(SO_4)_2$ –H_2O system at 25°C (A, B, points corresponding to $Na_2Cu(SO_4)_2 \cdot 2H_2O$ and $Na_2Mn(SO_4)_2 \cdot 2H_2O$, respectively).

= 983 cm^{-1}, ν_2 = 450 cm^{-1}, ν_3 = 1105 cm^{-1}, ν_4 = 611 cm^{-1} [20]. In solids the internal vibrations of the sulfate ions are expected to shift to lower or larger wavenumbers due to the interactions with other entitles in the structure.

$Na_2Cu(SO_4)_2 \cdot 2H_2O$ and $Na_2Mn(SO_4)_2 \cdot 2H_2O$ crystallize in the monoclinic space group (Z = 2; factor group symmetry C_{2h}) with 38 atoms in the unit cell and are characterized with 114 zone-center degrees of freedom. The SO_4^{2-} ions (four SO_4^{2-} ions in the unit cell located on C_1 sites) and the water molecules (four molecules in the unit cell located on C_1 sites) contribute 48 internal modes to the 114 optical zone-center modes – 36 internal modes for the tetrahedral ions and 12 internal modes for the water molecules).

The low site symmetry of the sulfate ions causes a removal of the degeneracy of both the doubly degenerate ν_2 modes and the triply degenerate ν_3 and ν_4 modes (the non-degenerate ν_1 mode is activated). According to the site symmetry analysis the nine internal modes of the tetrahedral ions are of A symmetry. Additionally, under the factor group symmetry C_{2h} each species of A symmetry splits into four components – Ag + Bg + Au + Bu (related to interactions of identical oscillators, correlation field effect; see correlation diagram in Fig. 4). Consequently, the 36 optical modes for the SO_4^{2-} ions are subdivided into 9Ag + 9Bg + 9Au + 9Bu modes. As was mentioned above the water molecules contribute 12 modes, as follows – 3Ag + 3Bg + 3Au + 3Bu.

The remaining 63 optical modes are distributed between the translational and librational lattice modes, as follows: 42 translations for (Na+, SO_4^{2-}, H_2O – all in C_1 site symmetry, Cu^{2+} – in C_i site symmetry; 9Ag + 9Bg + 12Au + 12Bu) and 24 librations (SO_4^{2-} and H_2O; 6Ag + 6Bg + 6Au + 6Bu).

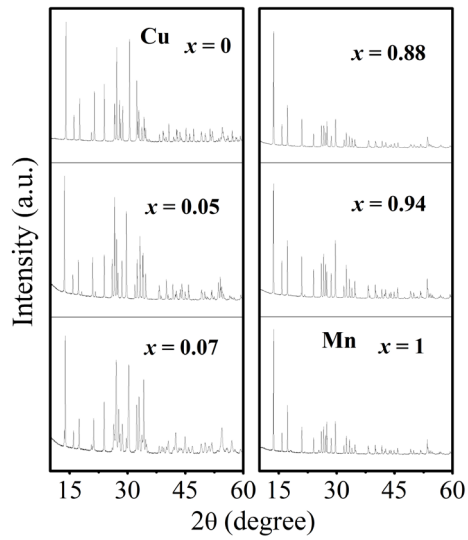

Fig. 3. X-ray powder diffraction patterns of $Na_2Cu(SO_4)_2 \cdot 2H_2O$, $Na_2Mn(SO_4)_2 \times 2H_2O$ and solid solutions $Na_2Cu_{1-x}Mn_x(SO_4)_2 \cdot 2H_2O$.

Thus, the 114 vibrational modes of the unit cell decompose, as follows:

Γ = 27Ag + 27Bg + 30Au + 30Bu; where 1Au + 2Bu are translations (acoustic modes).

Since the crystal structures of the kröhnkites are centrosymmetric, the Raman modes display g-symmetry,

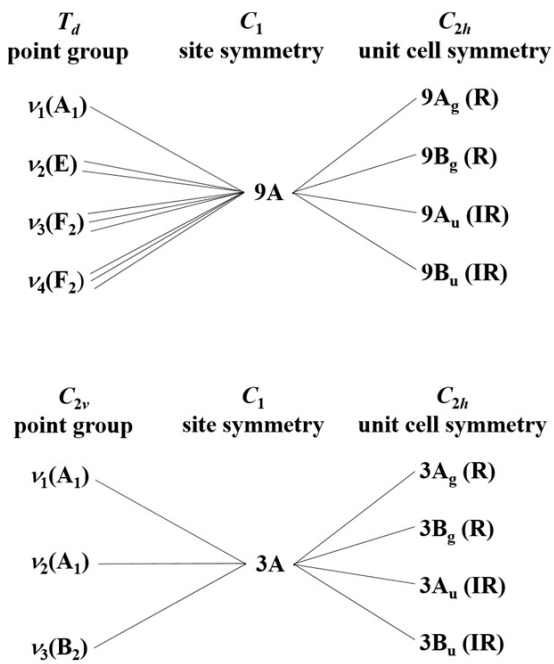

Fig. 4. Correlation diagrams between: T_d point symmetry, C_1 site symmetry and C_{2h} unit cell symmetry (SO_4^{2-} ions); C_{2v} point symmetry, C_1 site symmetry and C_{2h} unit cell symmetry (water molecules).

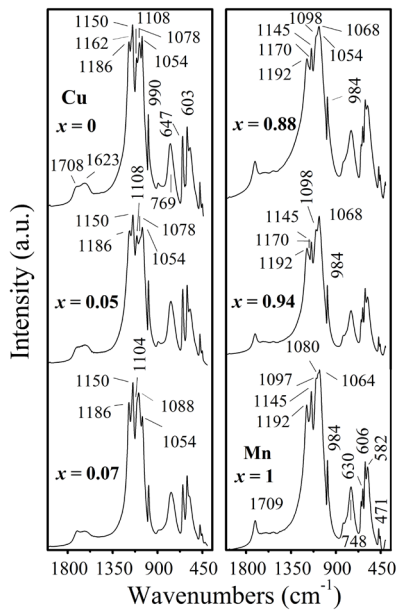

Fig. 5. Infrared spectra of solid solutions in the region of the normal vibrations of the sulfate ions, the bending modes of the water molecules and water librations.

and their IR counterparts display u-symmetry (mutual exclusion principle).

Raman and infrared spectra of $Na_2Cu(SO_4)_2 \cdot 2H_2O$ are commented briefly in Refs. [21 - 23] and those of $Na_2Mn(SO_4)_2 \cdot 2H_2O$ in Refs. [9, 16]. Fig. 5 shows infrared spectra of solid solutions $Na_2Cu_{1-x}Mn_x(SO_4)_2 \cdot 2H_2O$ in the region of the normal vibrations of the sulfate ions and water librations (for comparison the infrared spectra of the neat double hydrates are also given). Raman spectra of both kröhnkites are presented in Fig. 6. The assignments of the respective infrared and Raman bands are summarized in Table 3.

The analysis and the comparison of the vibrational spectra of the neat sulfate hydrates and solid solutions $Na_2Cu_{1-x}Mn_x(SO_4)_2 \cdot 2H_2O$ reveal:

(i) The ν_3 modes of the sulfate ions in both compounds are spread over wide spectral intervals thus indicating comparatively strong energetic distortions of the sulfate tetrahedra. $\Delta\nu_3$ calculated from the infrared spectra has values of 128 cm^{-1} and 132 cm^{-1} for the manganese and copper salts, respectively. This spectroscopic finding correlates with the geometric distortions of the tetrahedra – Δr has values of 0.031 and 0.035 Å for the tetrahedra in the manganese and copper compounds, respectively (Δr is the difference between the longest and the shortest bond length in the respective sulfate tetrahedra [3, 14]).

(ii) One interesting feature of the infrared spectra of both compounds is the grouping of the bands in the ν_3 region, thus confirming the conclusion that the sulfate tetrahedra are strongly energetically distorted (the bonds of the shorter S–O bond lengths, i.e. the stronger bonds have a considerable contribution to the bands at larger wavenumbers).

(iii) Another evidence for the strong energetic distortion of the sulfate ions in both compounds is the high intensity of the infrared bands corresponding to ν_1 (see Fig. 5). According to Petruševski and Šoptrajanov the intensity of the bands corresponding to ν_1 reflects the degree of distortion of the sulfate ions in series of salts – the higher the intensity of these bands is the stronger the geometric distortion of the polyatomic ions is [24].

(iv) The values of $\Delta\nu_3$ are larger than those of $\Delta\nu_4$, thus pointing that the sulfate ions are stronger distorted with respect to the S–O bond lengths as compared to the O–S–O bond angles (see Table 3).

(v) The appearance of more infrared and Raman bands corresponding to ν_3 than three bands expected according to the site symmetry analysis is owing to the interactions between the identical sulfate oscillators (crystal field effect). The larger number of the bands and the appearance of two bands for ν_1 in the Raman spectrum of the copper salt is a sign for the stronger crystal field effect on the sulfate vibrations in kröhnkite than that in Mn-kröhnkite due to the smaller unit cell volume of the copper compound (384.9 $Å^3$(Cu) vs. 399.9 $Å^3$(Mn)).

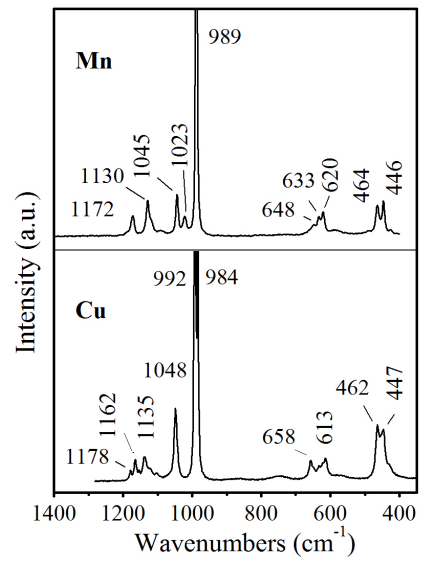

Fig. 6. Raman spectra of $Na_2Cu(SO_4)_2 \cdot 2H_2O$ and $Na_2Mn(SO_4)_2 \cdot 2H_2O$.

Table 3. Assignments of the vibrational modes in the region of 4000-400 cm^{-1} (normal vibrations of the sulfate tetrahedra, bending modes of water molecules, librations of water; ν_{OD} at liquid temperature are taken from Ref. [16]).

Vibrational mode	$Na_2Mn(SO_4)_2 \cdot 2H_2O$		$Na_2Cu(SO_4)_2 \cdot 2H_2O$	
	IR	Raman	IR	Raman
$\nu_3 O_W$	3208		3082	
$\nu_1 O_W$	3208		3082	
ν_{OD}	2392 2376		2371 2318	
$\nu_2 O_W$	1709		1623	
$\nu_3(SO_4)$	1192 1145	1172 1130	1186 1162	1178 1162
	1097 1080sh	1045 1023	1150 1108	1135 1120
	1064		1078 1054	1103 1048
$\nu_1(SO_4)$	984	989	990	992 984
ν(M–O)	823		892	
$L_R(H_2O)$	748		769	750
$L_W(H_2O)$	582		573	569
$\nu_4(SO_4)$	647 630 606	648 633 620	647 603	658 649
				639 633
				621 613
$\nu_2(SO_4)$	471 455	464 446	474 450	462 447

(vi) It is important to mention that the most of the infrared and Raman bands appear at different frequencies due to the different energy of the g- and u-motions (see Table 3).

(vii) The water librations (rocking and wagging) appear in the spectral region below 1000 cm^{-1}. The assignments of the bands are made by analogy to those for the Tutton compounds, $M'M''(XO_4)_2 \cdot 6H_2O$ (M' = K, Rb, Cs; M'' = Mg, Co, Ni, Cu, Zn; X = S, Se) [25 - 27]. Thus, the comparatively strong bands centered at 748 and 769 cm^{-1} and those at 582 cm^{-1} and 573 cm^{-1} originate from the rocking and wagging modes of the water molecules in the manganese and copper crystal hydrates, respectively. The appearance of the rocking modes for the copper compound at larger frequency as compared to those for the manganese one is an evidence for the formation of stronger hydrogen bonds in the former compound.

(viii) The hydrogen bonds in kröhnkite are stronger than those in Mn-kröhnkite as deduced from the bands corresponding to both the ν_{OH} and the ν_{OD} modes of matrix-isolated HDO molecules due to the stronger synergetic effect of the copper ions (see Table 3; the ν_{OD} motions ate taken from Ref. [21]). The data in Table 3 point also that the molecular symmetry of the water molecules in the manganese compound is close to C_{2v} ($\Delta\nu$ is 16 cm^{-1}), while $\Delta\nu_{OD}$ for the copper compound has a value of 53 cm^{-1}, i.e. the water molecules in kröhnkite demonstrate a considerable deviation from C_{2v} symmetry.

(ix) The inclusion of Cu^{2+} ions in the structure of Mn-kröhnkite changes the shape of the spectrum of the neat manganese compound: a new band (shoulder) at 1170 cm^{-1} appears in the spectrum of $Na_2Cu_{0.06}Mn_{0.94}(SO_4)_2 \cdot 2H_2O$ due to ν_3 of the sulfate ions coordinated to the included copper ions in [Cu–OSO_3] clusters. The lower frequency bands at 1057, 1080 and 1064 cm^{-1} (manganese compound) coalesce into two well-distinguished bands at 1098 and 1068 cm^{-1}. When the concentration of the copper ions in the solid solutions increases up to 12 mol % (sample $Na_2Cu_{0.12}Mn_{0.88}(SO_4)_2 \cdot 2H_2O$) a new shoulder at 1054 cm^{-1} arises, which is also owing to the included copper ions. The inclusion of Mn^{2+} ions in the copper compound

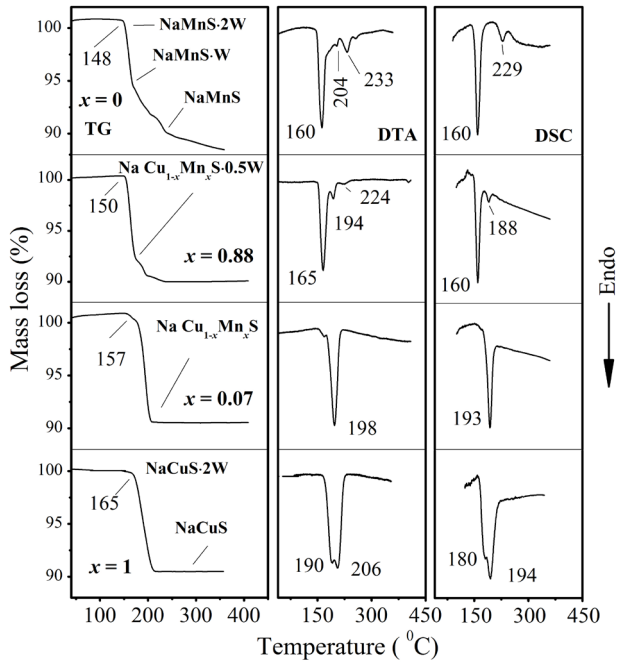

Fig. 7. TG, DTA and DSC curves of: $Na_2Cu(SO_4)_2 \cdot 2H_2O$, $Na_2Mn(SO_4)_2 \cdot 2H_2O$ and $Na_2Cu_{1-x}Mn_x(SO_4)_2 \cdot 2H_2O$.

also changes the profile of the spectra in the region of the lower wavenumbered components of ν_3: the band at 1054 cm^{-1} decreases in intensity and the bands at 1078 and 1108 cm^{-1} transform into one intensive band at 1088 cm^{-1} and a shoulder at 1004 cm^{-1} (see the spectrum of the sample $Na_2Cu_{0.93}Mn_{0.07}(SO_4)_2 \cdot 2H_2O$). The lower frequency parts of the spectra of the host compounds (regions of ν_4, ν_1 and water librations) are not influenced by the copper and manganese guest ions.

Thermal behavior and phase transitions

The anhydrous sodium manganese sulfate is reported to form two minerals known as alluaudite ($Na_2Mn_2(SO_4)_3$) and vanthoffite ($Na_6Mn(SO_4)_4$) [9, 28, 29]. The mass loss behavior of Mn-kröhnkite is commented briefly in a previous paper of one of the authors (DM). The thermal dehydration occurs stepwise, thus forming a monohydrate as an intermediate product with an alluaudite-type structure [9]. $Na_6Mn(SO_4)_4$ (M = Mg, Mn, Fe, Co, Ni, Zn) with a vanthoffite-type structure (monoclinic space group $P2_1/c$) are reported to crystallize from Na_2SO_4–MSO_4 systems. The copper analog was not synthesized [28]). Recently, Sharma et al. prepared single crystals of $Na_6Mn(SO_4)_4$ by crystallization from an aqueous solution containing a 3:1 molar ratio of Na_2SO_4 and $MnSO_4 \cdot H_2O$ at 80°C and solved its crystal structure. It crystallizes in the monoclinic SG $P2_1/c$ (a = 9.6910(5) Å; b = 9.281(5) Å; c = 8.258(5) Å; β = 113.124(5)º; V = 683.1(7) $Å^3$, Z = 2) [29]. Alluaudite crystallizes in the monoclinic SG $C2/c$ (a = 12.764(1) Å; b = 12.943(1) Å; c = 6.5871(6) Å; β = 115.780(3) º; V = 979.95(25) $Å^3$; Z = 4) [9].

The literature data concerning the dehydration of kröhnkite are contradictory. According to Silber and Cot the dehydration of $Na_2Cu(SO_4)_2 \cdot 2H_2O$ occurs in one step, thus forming two polymorphic modifications of the anhydrous product [30]. Nagase and Yokobayashi reported that $Na_2Cu(SO_4)_2 \cdot H_2O$ is obtained as an intermediate product [31]. Recently, the anhydrous sodium copper sulfate $Na_2Cu(SO_4)_2$ (mineral saranchinaite) has been found in sublimates of the Saranchinaitovaya fumarole, Naboko Scoria Cone, Tolbachik volcano, Kamchatka (Russia). It crystallizes in monoclinic space group $P2_1$ with lattice parameters: a = 9.0109(5) Å, b = 15.6355(8) Å, c = 10.1507(5) Å, β = 107.079(2)º, V = 1367.06(12) $Å^3$, Z = 8. The authors provided results for the preparation of the anhydrous compound by heating kröhnkite at 200ºC using a HTXRD method [32]. Testasicca et al. reported that kröhnkite is stable up to 150ºC and forms a mixture of copper and sodium sulfates at higher temperature. The authors do not comment the formation of an anhydrous sodium copper sulfate [33]. Our previous experimental results from TG, DTA and DSC analyses show that the escape of the water molecules from kröhnkite occurs in one step. This finding was confirmed with X-ray diffraction at elevated temperature – kröhnkite exists up to 250ºC according to our experiments and loses completely the water molecules at about 300ºC. The enthalpy of dehydration of $Na_2Cu(SO_4)_2 \cdot 2H_2O$ has a value of 354.0 kJ mol^{-1} and that of formation -2996.5 kJ mol^{-1} [2].

TG–DTA–DSC curves of solid solutions $Na_2Cu_{1-x}Mn_x(SO_4)_2 \cdot 2H_2O$ and neat double salts are shown in Fig. 7. Several inflexion points are observed on the TG curve of the manganese kröhnkite at about 168, 206 and 238ºC. The first inflexion point corresponds to the loss of 6.48 % of the weight, the second to the 2.58 % and the third to 1.72 %. Thus, the total dehydration of the manganese compound completes at about 236ºC (Δm_{cal} = 10.94 mass %; Δm_{exp} = 10.78 mass %). The process of dehydration is registered on the DTA curve with one intensive endoeffect at 160ºC and two weak endoeffects at 204 and 233ºC. At temperatures higher

than 240ºC a process of decomposition of the manganese kröhnkite probably begins. It is important to mention that all these processes occur continuously as TG curve shows (no intervals of stability of intermediate products are observed). DSC curve is characterized with two endoeffects at 160 and 229ºC. ΔH_{deh} calculated for the first intensive effect has value of 363.6 kJ mol^{-1}. ΔH_{deh} for the two water molecules has value of 394.7 kJ mol^{-1} and ΔH_f of $Na_2Mn(SO_4)_2 \cdot 2H_2O$ is -3368.3 kJ mol^{-1}. The included Cu^{2+} ions in the crystals of Mn-kröhnkite

Table 4. X-ray powder diffraction data of saranchinaite prepared after heating kröhnkite at 350ºC for two days (in Å for CuKα).

hkl	d_{calc}	d_{exp}	I/I_{0exp}	*hkl*	d_{calc}	d_{exp}	I/I_{0exp}
100	8.5868	8.6016	72	-113	3.2956	3.2966	37
011	8.2349	8.2458	37	003	3.2358	3.2346	38
020	7.7761	7.7947	100	013	3.1680	3.1664	14
-101	7.6404	7.6468	89	-123	3.0938	3.0925	25
021	6.0690	6.0680	38	-203	3.0501	3.0595	23
111	5.3185	5.3178	17	-302	2.8601	2.8698	21
-102	4.8840	4.8835	49	-302	2.8601	2.8596	30
002	4.8537	4.8576	46	-312	2.8130	2.8131	44
012	4.6333	4.6339	52	212	2.7842	2.7839	23
121	4.5760	4.5767	48	151	2.7259	2.7259	60
-201	4.4380	4.4375	15	142	2.7091	2.7096	81
022	4.1174	4.1184	32	-104	2.5385	2.5386	48
040	3.8880	3.8875	15	311	2.5163	2.5165	20
-202	3.8202	3.8202	27	160	2.4814	2.4825	15
-220	3.7586	3.7588	97	-214	2.4125	2.4125	14
-140	3.5419	3.5422	41	-243	2.3998	2.4001	17
-141	3.4652	3.4658	15	-411	2.2164	2.2160	3
-222	3.4288	3.4286	5	170	2.1509	2.1511	3
-230	3.3066	3.3053	5				

change the profiles of the TG curve. The dehydration of $Na_2Cu_{0.12}Mn_{0.88}(SO_4)_2 \cdot 2H_2O$ begins at about 150ºC and completes at about 230ºC, thus forming an anhydrous solid solution. The first inflexion point on the TG curve of the sample $Na_2Cu_{0.12}Mn_{0.88}(SO_4)_2 \cdot 2H_2O$ at 177ºC corresponds to the loss of 7.86 mass %, thus producing $Na_2Cu_{0.12}Mn_{0.88}(SO_4)_2 \cdot 0.5H_2O$ (the theoretical mass loss is 8.21 mass %). The full separation of the crystallization water occurs at about 230ºC (theoretical mass loss is 10.94 mass%; experimental - 9.60 mass %). The process of dehydration is registered on the DTA curve with three endothermic peaks – one intensive peak centered at 165ºC related to the release of 1.5 water molecules and two weak endoeffects at 194 and 224ºC. DSC measurements show that the total ΔH_{deh} of $Na_2Cu_{0.12}Mn_{0.88}(SO_4)_2 \cdot 2H_2O$ is 402.2 kJ mol^{-1} (372.5 kJ mol^{-1} for the removal of 1.5 water molecules and 29.7 kJ mol^{-1} for the separation of the last 0.5 water molecules). ΔH_f of $Na_2Cu_{0.12}Mn_{0.88}(SO_4)_2 \cdot 2H_2O$ has value of -3336 kJ mol^{-1}.

The sample $Na_2Cu_{0.93}Mn_{0.07}(SO_4)_2 \cdot 2H_2O$ displays a TG curve identical with that of kröhnkite. The two intensive peaks at 190 and 206ºC on the DTA curve of the copper salt coalesce into one peak at 198ºC on the DTA curve of the solid solution. According to DSC measurements (peak maximum at 193ºC) ΔH_{deh} and ΔH_f of $Na_2Cu_{0.93}Mn_{0.07}(SO_4)_2 \cdot 2H_2O$ have values of 329.6 kJ mol^{-1} and -2987 kJ mol^{-1}, respectively, values which are close to those for the neat $Na_2Cu(SO_4)_2 \cdot 2H_2O$ (see above in the text).

Anhydrous solid solutions were prepared by heating the hydrates at 350ºC for two days. The X-ray diffraction patterns of anhydrous compounds prepared from $Na_2Cu(SO_4)_2 \cdot 2H_2O$ and $Na_2Cu_{1-x}Mn_x(SO_4)_2 \cdot 2H_2O$ (x = 0.05, 0.07) are shown in Fig. 8 (the pattern of saranchinaite according to [32] is also presented; see Fig. 8a). The pattern of the $Na_2Cu(SO_4)_2 \cdot 2H_2O$ heated at 350 ºC shows reflections of an unidentified phase (or phases) (reflections marked with asterisks; Fig. 8b) additionally to the saranchinaite-phase. The lattice parameters calculated for SG $P2_1$ have the following values: a = 8.983(4) Å; b = 15.552(7) Å; c = 10.155(2) Å; β = 107.07(3)º; V = 1356.1 Å^3. The sample $Na_2Cu_{0.95}Mn_{0.05}(SO_4)_2 \cdot 2H_2O$ exhibits a diffractogram identical to that of saranchinaite (Fig. 8c). New additional reflections appear in the diffraction pattern of this anhydrous sample (Fig. 8d). The lattice parameters of the anhydrous sample are: a = 9.0224 Å; b = 15.5625 Å; c = 10.1601 Å; β = 107.43º; V = 1361.1 Å^3. The slight increase in the lattice parameters of the anhydrous solid solution as compared to those of pure saranchinaite is in agreement with the larger ionic radius of the guest manganese ions.

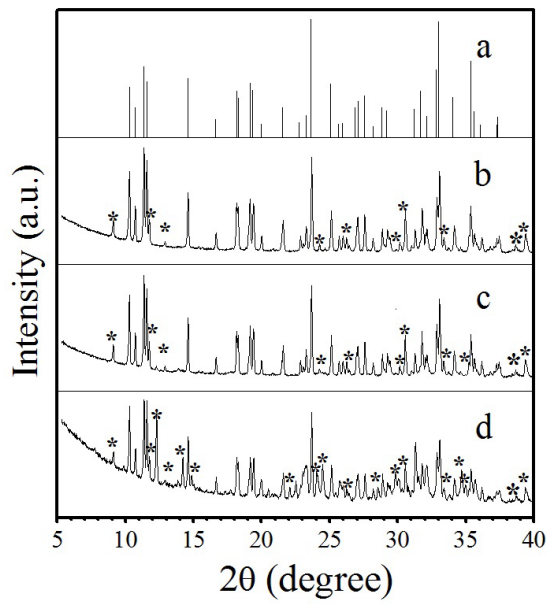

Fig. 8. X-ray powder diffraction patterns of:
a) saranchinaite according to Ref. [32]; b) $Na_2Cu(SO_4)_2$; c) $Na_2Cu_{0.95}Mn_{0.05}(SO_4)_2$; d) $Na_2Cu_{0.93}Mn_{0.07}(SO_4)_2$ (asterisks, unidentified phases).

The phase transitions of the solid solutions having as a matrix the copper compound were monitored also by means of X-ray diffraction at elevated temperature (reflections of new phase are marked with asterisks). Fig. 9a shows that kröhnkite is stable up to 250ºC and at 300ºC it transforms into anhydrous compound with a saranchinaite-type structure. The solid solution $Na_2Cu_{0.93}Mn_{0.07}(SO_4)_2 \cdot 2H_2O$ preserves the crystal structure of kröhnkite up to 250ºC and of saranchinaite at higher temperature (Fig. 9b). The comparison of Figs. 8b and 9a, allows us to assume that the longer heating time favors the decomposition of kröhnkite.

The inclusion of Cu^{2+} ions in the structure of Mn-kröhnkite yields anhydrous solid solutions with an alluaudite-type structure and a new phase (see Fig. 10). Marinova et al. reported that the solid solution $Na_2Co_{0.63}Mn_{0.37}(SO_4)_2 \cdot 4H_2O$ heated at 350 ºC for 40 h transforms into two phases - solid solutions $Na_2(Co/Mn)_2(SO_4)_3$ with an alluaudite-type structure and solid solutions $Na_6(Co/Mn)(SO_4)_4$ with a vanthoffite-type structure [11]. Thus, the new phase formed after heating the solid solutions reached in manganese is vanthoffite

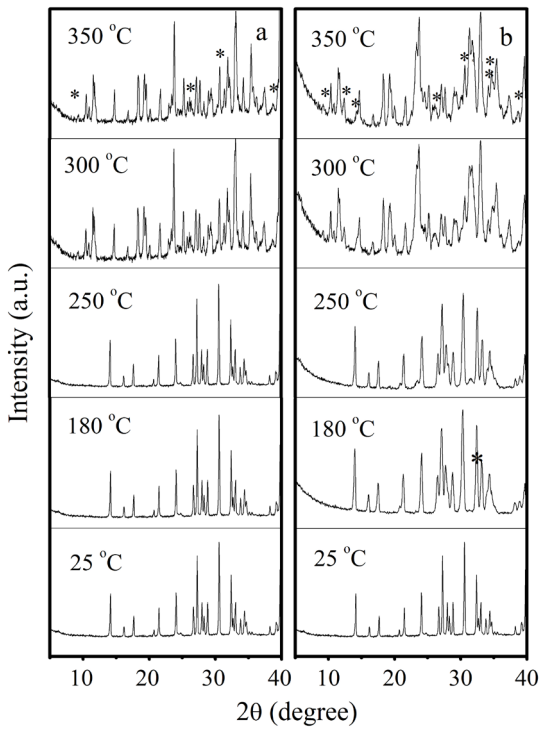

Fig. 9. Evolution of the X-ray patterns at elevated temperature of: a) $Na_2Cu(SO_4)_2 \cdot 2H_2O$ and b) $Na_2Cu_{0.93}Mn_{0.07}(SO_4)_2 \cdot 2H_2O$ (asterisks, unidentified phases).

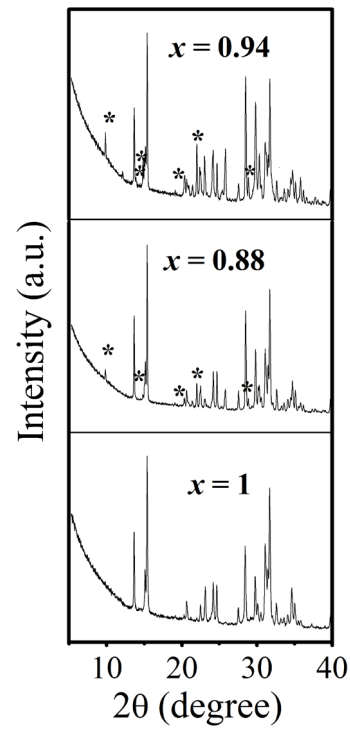

Fig. 10. X-ray powder diffraction patterns of $Na_2Mn(SO_4)_3$ and $Na_2Cu_{1-x}Mn_x(SO_4)_2$ (x = 0.94 and 0.88; asterisk, vanthoffite phase).

$Na_6Mn(SO_4)_4$ (marked with asterisks). The lattice parameters of the solid solution with an alluaudite-type structure obtained by heating $Na_2Cu_{0.12}Mn_{0.88}(SO_4)_2 \cdot 2H_2O$ have values of: a = 12.808(8) Å; b = 12.951(7) Å; c = 6.567(3) Å; β = 115.91(5)º; V = 980.1 Å^3.

Fig. 11 shows the morphology of the kröhnkites (Fig. 11a, c) and of respective anhydrous compounds (Figs. 11b and d). The measurements reveal that the difference in the shape of the particles of the hydrated salts and the corresponding anhydrous analogs is negligible.

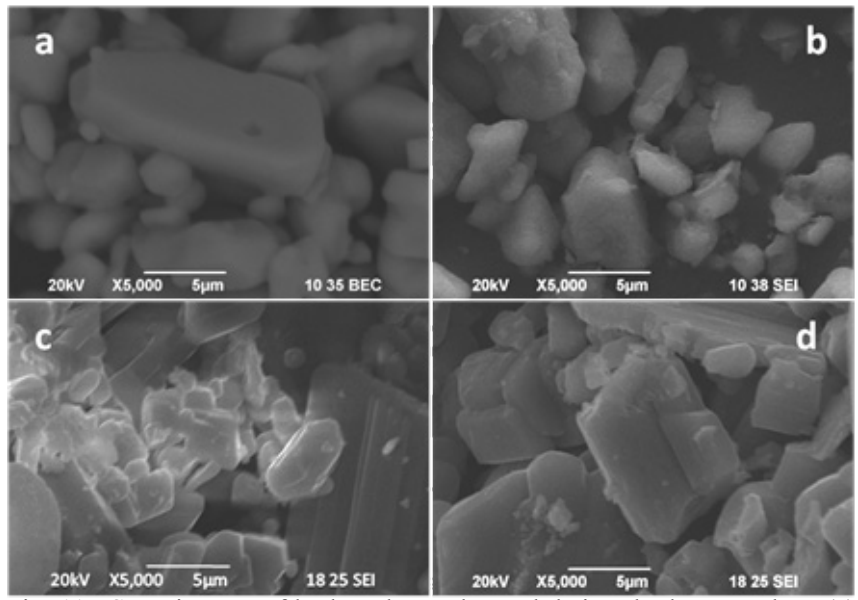

Fig. 11. SEM images of hydrated samples and their anhydrous analogs (a) $Na_2Cu(SO_4)_2 \cdot 2H_2O$; b) $Na_2Cu(SO_4)_2$; c) $Na_2Mn(SO_4)_2 \cdot 2H_2O$; d) $Na_2Mn(SO_4)_3$).

All samples consist of isometric to slightly oval shaped particles. The particles size varies in a large range from 1.3 to 16.2 μm. The determination of the grain sizes is made by intercept line method (program Lince Liner Intercept 2.4.2e).

CONCLUSIONS

Two types of solid solutions of a kröhnkite-type structure are formed in the system kröhnkite – Mn-kröhnkite – water, irrespective of the isostructureness of the salts due to the different ionic radii of the metal ions (0.73(Cu) vs. 0.83(Mn)), different lattice parameters and the Jahn-Teller effect. The distribution coefficient of the manganese ions between the liquid phases and solid solutions $D_{Mn/Cu}$ has a mean value 0.04, while $D_{Cu/Mn}$ has a mean value of 0.66.

The vibrational spectra reveal that the ν_3 modes of the sulfate tetrahedra in both compounds are spread over wide spectral ranges, thus indicating a strong deviation of the sulfate ions from T_d symmetry in agreement with the structural data. The stronger Cu–OSO_3 bonds and the smaller unit cell volume of the copper compound (384.9 $Å^3$(Cu) vs. 399.9 $Å^3$(Mn)) lead to a stronger sulfate ion distortion in the copper compound as compared to that of the sulfate tetrahedra in the manganese one. The hydrogen bonds in kröhnkite are stronger than those in Mn-kröhnkite due to the stronger Cu–O_W interactions, i.e. to the stronger synergetic effect of the copper ions. The appearance of more vibrational bands corresponding to ν_3 than three bands expected according to the site symmetry analysis is owing to the strong crystal field effect.

TG-DTA-DSC analyses reveal that the thermal dehydration of the solid solution $Na_2Cu_{0.12}Mn_{0.88}(SO_4)_2 \cdot 2H_2O$ forms as an intermediate product $Na_2Cu_{0.12}Mn_{0.88}(SO_4)_2 \cdot 1.5H_2O$, while the solid solution $Na_2Cu_{0.93}Mn_{0.07}(SO_4)_2 \cdot 2H_2O$ transforms directly into an anhydrous salt. Solid solutions having a copper compound as a matrix form after heating at 350ºC anhydrous solid solutions with a saranchinaite-type structure and unidentified solid phase or phases. The solid solutions having a manganese sulfate as a matrix also yield after complete dehydration two phase systems – solid solutions with an alluaudite-type structure and a solid phase with a vanthoffite-type structure, $Na_6Mn(SO_4)_4$.

Acknowledgements

The financial support from the Scientific Research Department of the University of Chemical Technology and Metallurgy (Republic of Bulgaria) is acknowledged (Project No. 11712/2017).

REFERENCES

1. M. Georgiev, Tsv. Bancheva, D. Marinova, R. Stoyanova, D. Stoilova, On the formation of solid solutions with blödite- and kröhnkite-type structures. I. Synthesis, vibrational and EPR spectroscopic investigations of $Na_2Zn_{1-x}Cu_x(SO_4)_2 \cdot 4H_2O$ ($0 < x < 0.14$), I. J. Sci. Res. Sci. Technol., 2, 5, 2016, 279-292.
2. D. Marinova, M. Georgiev, Tsv. Bancheva, D. Stoilova, On the formation of solid solutions with blödite - and kröhnkite-type structures. II. Structural and Thermal Investigations of Solid Solutions $Na_2Zn_{1-x}Cu_x(SO_4)_2 \cdot 4H_2O$ ($0 < x < 0.14$), I. J. Sci. Res. Sci. Technol., 2, 6, 2016, 283-295.
3. D. Marinova, M. Georgiev, Tsv. Bancheva, R. Stoyanova, D. Stoilova, On the formation of solid solutions with blödite- and kröhnkite-type structures. III. Synthesis, structural, thermal and spectroscopic investigations of $Na_2Ni_{1-x}Cu_x(SO_4)_2 \cdot 4H_2O$, J. Therm. Anal. Calorim., 130, 2017, 1925-1937.
4. D. Marinova, M. Wildner, Tsv. Bancheva, R. Stoyanova, M. Georgiev, D. Stoilova, Synthesis, structure and properties of blödite-type solid solutions, $Na_2Co_{1-x}Cu_x(SO_4)_2 \cdot 4H_2O$ ($0 < x \leq 0.18$), and crystal structure of synthetic kröhnkite, $Na_2Cu(SO_4)_2 \cdot 2H_2O$. Phys. Chem. Minerals, 45, 2018, 801-817.
5. M. Georgiev, D. Marinova, Tsv. Bancheva, D. Stoilova, On the formation of solid solutions with blödite- and kröhnkite-type structures. IV. Synthesis, structural, spectroscopic and thermal investigations of $Na_2Co_{1-x}Mg_x(SO_4)_2 \cdot 4H_2O$ ($0 < x < 1$). J. Chem. Tech. Metal., 52, 2017, 902-917.
6. D.M. Marinova, E.N. Zhecheva, R.R. Kukeva, P.V. Markova, D.D. Nihtianova, R.K. Stoyanova, Mixed sodium nickel-manganese sulfates: Crystal structure relationships between hydrates and anhydrous salts. J. Solid State Chem., 250, 2017, 49-59.
7. M. Reynaud, Design of new sulfate-based positive electrode materials for Li- and Na-ion batteries, Material chemistry, Ph.D. Thesis, Université de

Picardie Jules Verne, France, 2013, English version.
8. M. Reynaud M, S. Ati M. Boulineau, M.T. Sougrat, B.C. Melot BC, G. Rousse, J.N. Chotard, J.M.Tarasco, Sulfates $A_2M(SO_4)_2 \cdot nH_2O$ (A = Li, Na and M = Transition Metal): as New Attractive Electrode Materials for Li- and Na-Ion Batteries. ECS Transact., 50, 2013, 11-19.
9. D. Marinova, V. Kostov, R. Nikolova, R. Kukeva, E. Zhecheva, M. Sendova-Vasileva, R. Stoyanova, From kröhnkite- to alluaudite-type of structure: novel method of synthesis of sodium manganese sulfates with electrochemical properties in alkali-metal ion batteries. J. Mater. Chem., 3A, 1915, 22287-22299.
10. D. Marinova, R. Kukeva, E. Zhecheva, R. Stoyanova, Selective Sodium Intercalation into Sodium Nickel-Manganese Sulfate for Dual Na-Li-Ion Batteries. Phys. Chem. Chem. Phys., 2018, 20, 2018, 12755-12766.
11. D.M. Marinova, V.V. Kostov, R.P. Nikolova, R.R. Kukeva, E.N. Zhecheva, R.K. Stoyanova, Redox properties of alluaudite sodium cobalt manganese sulfates as high-voltage electrodes for rechargeable batteries. Chem. Commun., 43, 2018, 5466-5469.
12. M. Fleck, U. Kolitsch, B. Hertweck, Natural and synthetic compounds with kröhnkite-type chains: review and classification. Z. Kristallogr. NCS, 217, 2002, 1-9.
13. M. Fleck, U. Kolitsch, Natural and synthetic compounds with kröhnkite-type chains. An update. Z. Kristallogr. NCS, 218, 2003, 553-567.
14. M. Wildner, D. Stoilova, Crystal structures and crystal chemical relationships of kröhnkite-and collinsite type compounds $Na_2Me(XO_4)_2.2H_2O$ (X = S, Me = Mn, Cd; X = Se, Me=Mn, Co, Ni, Zn, Cd) and $K_2Co(SeO_4)_2 \cdot 2H_2O$. Z. Kristallogr., 218, 2003, 201-209.
15. M. Wildner, On the geometry of $Co(II)O_6$ polyhedra in inorganic compounds. Z. Kristallogr., 202, 1992, 51-70.
16. D. Stoilova, M. Wildner, V. Koleva, Infared study of ν_{OD} modes in isotopically dilute (HDO molecules) $Na_2Me(XO_4)_2 \cdot 2H_2O$ with matrix-isolated $X'O_4^{2-}$ guest ions (Me = Mn, Co, Ni, Cu, Zn, Cd; X – S, Se). J. Mol. Struct., 643, 2002, 37-41.
17. V.B. Kogan, C.K. Ogorodnikov, V.V. Kafarov, Ternary and Polycomponent Systems of Inorganic Compounds. Izd. Nauka, Leningrad, v. 3, 1970.
18. Chr. Balarew, V. Karaivanova, T. Oikova, Contribution to the study of the isomorphic and isodimorphic inclusions in crystal salts. III. Examination of the systems zinc sulfate-cobalt sulfate-water and zinc sulfate water- nickel sulfate-water at 25°C. Chem. Commun. Departm. Bulg. Acad Sci., 3, 1970, 673-684.
19. D. Trendafelov, Chr. Balarew, Beitrag sur Untersuchung der isomorphen und isodimorphen Einschlusse in Kristallsalzen. II. Untersuchung der Verteiligung der Kobaltionen in verschiedenen Zinksulfathydraten. Commun. Dept. Chem. Bulg. Acad. Sci., 1968, 1, 73-80.
20. K. Nakamoto, Infrared and Raman spectra of Inorganic and Coordination Compounds, John Wiley & Sons, New York, 1986.
21. D. Stoilova, M. Wildner, V. Koleva, Vibrational behavior of the S–O stretches in compounds with kröhnkite-type chains $Na_2Me(SeO_4)_2 \cdot 2H_2O$ with matrix-isolated SO_4^{2-} and M'^{2+} guest ions (Me= Mn, Co, Ni, Cu. Vib. Spectrosc., 1, 2003, 115-123.
22. V.P.M. Pillai, V.U. Nayar, V.B. Jordanovska, Infrared and Raman spectra of $Na_2Cu(SO_4)_2 \cdot 2H_2O$ and $CH_3NH_3 \cdot 2M(II)(SO_4)_2 \cdot 6H_2O$ with M(II) = Cu, Xn, and Ni. J. Solid State Chem., 133, 1997, 407-415.
23. R.L. Frost, Y. Hi, R. Scholz, Vibrational Spectroscopy of the Copper (II) Disodium Sulphate Dihydrate Mineral Kröhnkite $Na_2Cu(SO_4)_2 \cdot 2H_2O$. Spectrosc. Lett., 46, 2013, 447-452.
24. V. Petruševski, B. Šoptrajanov, Description of molecular distortions. II. Intensities of molecular distortions II. Intensities of the symmetric stretching bands of tetrahedral molecules. J. Mol. Struct., 175, 1988, 349-354.
25. J.A. Campbell, D.P. Ryan, L.M. Simpson, Interionic forces in crystal-II. Infrared spectra of SO_4 groups and 'octahedrally' coordinated water in some alums, Tutton salts, and the double salts obtained by dehydrating them. Spectrochim. Acta, 26A, 1970, 2351-2361.
26. Zd. Mička, L. Prokopová, I. Cisařová, D. Havliček,

Crystal structure, thermoanalytical properties and infrared spectra of double magnesium selenates. Crystal structure, thermoanalytical properties and infrared spectra of double magnesium selenates. Collect. Czech. Chem. Commun., 61, 1996, 1295-1306.

27. M. Wildner, D. Marinova, D. Stoilova, Vibrational spectra of $Cs_2Cu(SO_4)_2 \cdot 6H_2O$ and $Cs_2Cu(SeO_4)_2 \cdot nH_2O$ (n = 4, 6) with a crystal structure determination of the Tutton salt $Cs_2Cu(SeO_4)_2 \cdot 6H_2O$. J. Mol. Struct., 1106, 2016, 440-451.
28. K.L. Keester, W. Eysel, New compounds $MNa_6(SO_4)_4$ with vanthoffite structure. Acta Crystallogr., B33, 1977, 306-307.
29. V. Sharma, D. Swain, T.N. Curu Row, Superrionic Behavior and Phase Transition in a Vanthoffite Mineral. Inorg. Chem., 56, 2017, 6048-6051.
30. P. Silber, M.L. Cot, Sur quelques proprietes de l'espece cristalline $Na_2Cu(SO_4)_2$ et de son hydrate $Na_2Cu(SO_4)_2 \cdot 2H_2O$. C. R. Acad. Sc. Paris, Ser. C., 1967, 312-315.
31. K. Nagase, H. Yokobayashi, Spectrometric and thermal analytical studies on the dehydration of copper(II) sulfate and its double salts. Thermochim. Acta, 23, 1978, 283-291.
32. O.I. Siidra, E.A. Lukina, E.V. Nazarchuk, W. Depmeier, R.S. Bubnova, A.A. Agakhanov, E.Y. Adontseva, S.K. Filatov, V.M. Kovrugin, Saranchinaite, $Na_2Cu(SO_4)_2$, A New Exhalative Mineral from Tolbachik Volcano, Kamchatka, Russia, and a product of the Reversible Dehydration of Kröhnkite, $Na_2Cu(SO_4)_2(H_2O)_2$. Mineral. Mag., 82, 2018, 257-274.
33. L.P. Testasicca, R.I. Frost, X. Ruan, J.I. Lima, The application of high-temperature X-ray diffraction and infrared emission spectroscopy to the thermal decomposition of kröhnkite. J. Therm. Anal. Calorim., 126, 2016, 1089-1095.